Modelling of plasma environment of Cluster electrostatic sensors

A. Hilgers, B. Thiébault, J. Forest, A. Masson, P. Escoubet, H. Laakso, J-F Roussel etc…
European Space Agency (ESTEC/TEC-EES)

- Photo-electron environment
- Double probe model for estimate of density and temperature
- PicUp3D
- SPIS

Table: 3 Parameters for Cluster spacecraft simulations

Cluster parameters

Parameter	Value
Electron and ion temperature	100 eV
Photo-electron temperature	1.5 eV
Photo-electron current density	30 $\mu A\ m^{-2}$
Plasma number density	1.0 cm^{-3}
Debye length	74 m
Spacecraft potential	0.0 to 7.0 V
Spacecraft radius	1.41 m

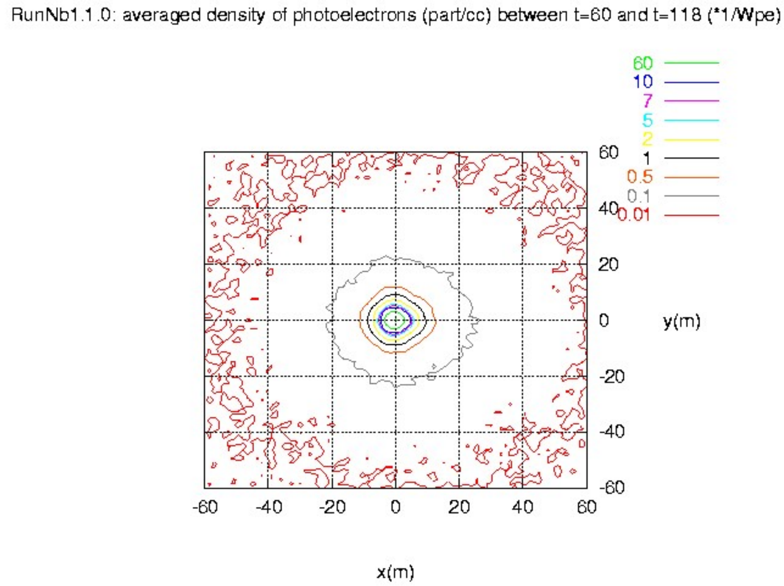

PIC simulation of half-emitting spacecraft (Thiébault et al., 2005)

Turning point method description (1)

- Based on Parrot et al. [1982]
- Solving the Vlasov-Poisson system iteratively around a spherical probe in an infinite plasma

$$\Delta_R \Phi(R) = -\frac{\rho(R)}{\epsilon_0} \qquad V_i.\nabla f_i - q_i \nabla\Phi.\nabla_p f_i = 0$$

- Plasma composed of ions, electrons and photoelectrons
- Plasma is assumed to be stationary, collisionless
- In unperturbed plasma, ions and electrons distribution functions are assumed Maxwellian
- Plasma conditions independent of time and not influenced by magnetic field

Turning point method description (2)

Each number density is calculated as a function of the radial distance and the potential distribution via the identification of the domain of accessibility in function of momentum *l* and energy ε:

$$n_i(r) = \frac{2\alpha_i \cdot \exp(\phi_{i,S})}{\sqrt{\pi}} \int_{\phi_{i,S}}^{\infty} \exp(-\epsilon_i) M_{n_i}(\epsilon_i) d\epsilon_i,$$

where

$$M_{n_i}(\epsilon_i) = \sum_j \xi_j \left[K_{n_i}(l_i^2)\right]_{(l_i^2)_{\min_j}}^{(l_i^2)_{\max_j}},$$

with

$$K_{n_i}(l_i^2) = \frac{1}{2r}\sqrt{g_i(r) - l_i^2}$$

and

$$g_i(r) = r^2(\epsilon_i - \phi_i).$$

Turning point method description (3)

- Orbit classification using the turning point formulation used to solve the expression of the density

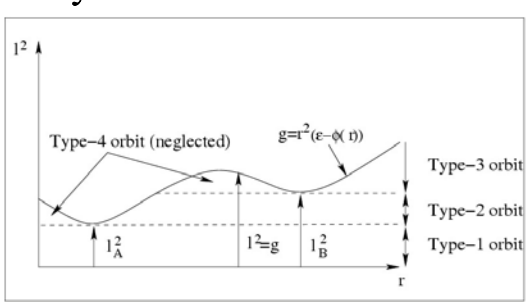

Example of space charge effect in non-limiting regime *(Thiébault et al., 2004)*

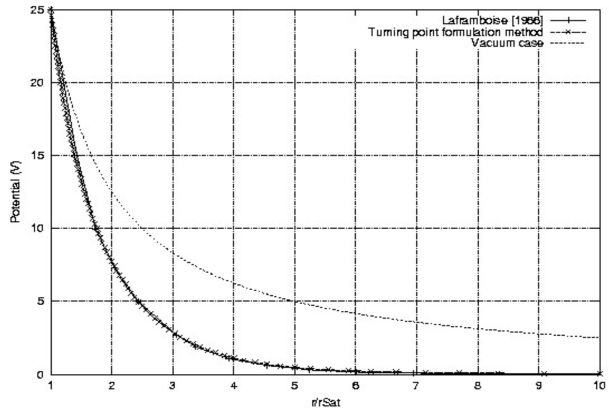

Validation of PicUp3D with uniform photo-emission

- Comparison TP-PicUp3D (100 cc, 1 eV)

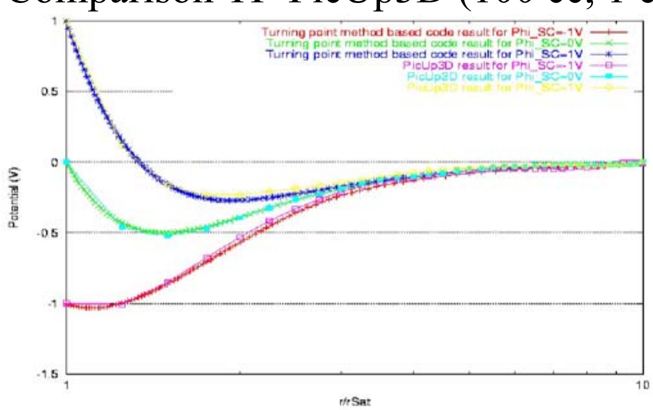

Example of non-uniform photo-emission effect *(Thiébault et al., JGR, 2004)*

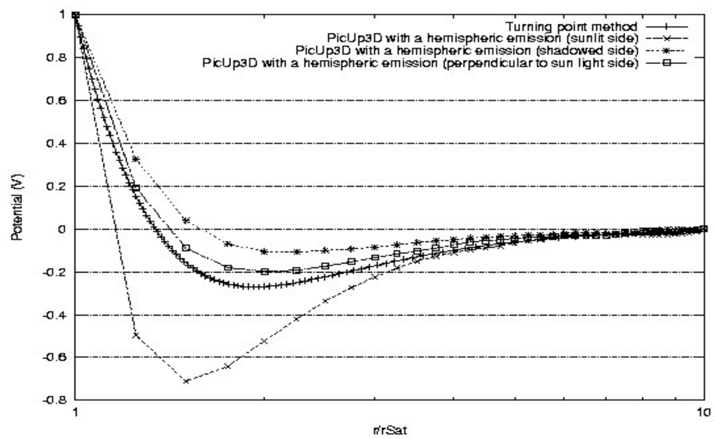

T= 1 eV
N= 100 cm-3

SPINE, 13-14 Nov. 2008, ESTEC

Potential barrier height Φ_B (left panel) and location (right panel) versus Cluster spacecraft potential computed with the turning point method.

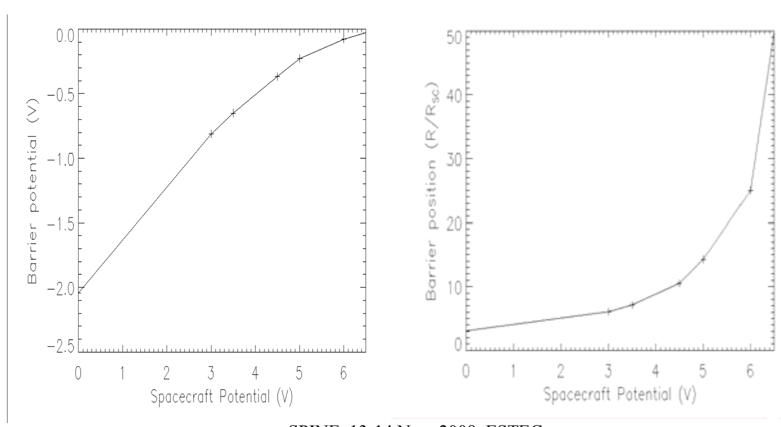

SPINE, 13-14 Nov. 2008, ESTEC

Comparison with Geotail data (1)

- Geotail observation (Zhao et al.[1996])
  - Current equation to assess the value of the potential barrier

$$J_{ph}(1+\Delta u)exp(-\Delta u)\frac{S}{4\pi R^2} = J_e\Big(1+\frac{T_{ph}}{T_e}\Delta u\Big)\cdot exp\Big(-\frac{T_{ph}}{T_e}\Delta u\Big)\cdot exp\Big(-\frac{T_{ph}}{T_e}u_s\Big)+\frac{I}{4\pi R^2}$$

  - Predefined parameterised potential profile to provide a potential barrier location
  - Other hypotheses :
    - Spherical symmetry
    - Ion and electron temperature : 100 eV
    - Plasma density : 1 cm^{-3}

Comparison with Geotail data (2)

- Predicted potential minimum with the turning point formulation

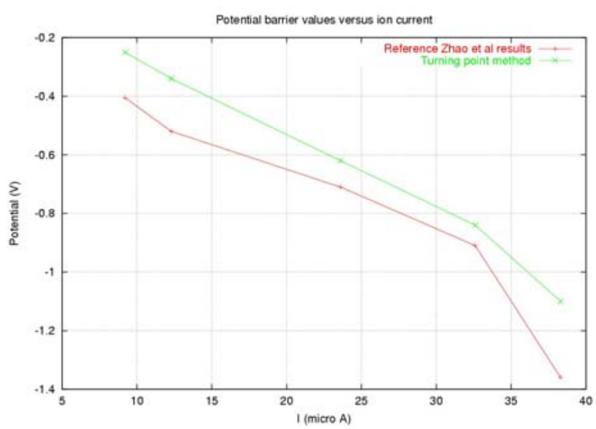

Comparison with Geotail data (3)

- Predicted barrier position with the turning point formulation

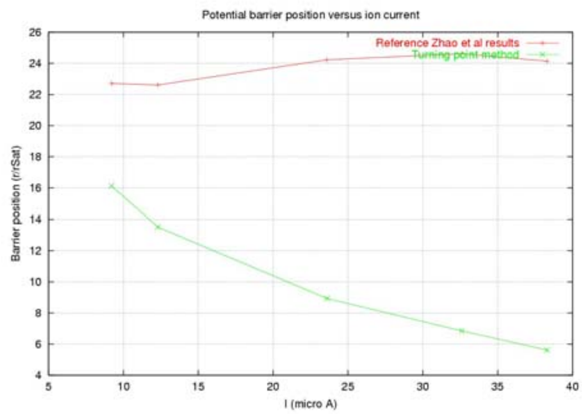

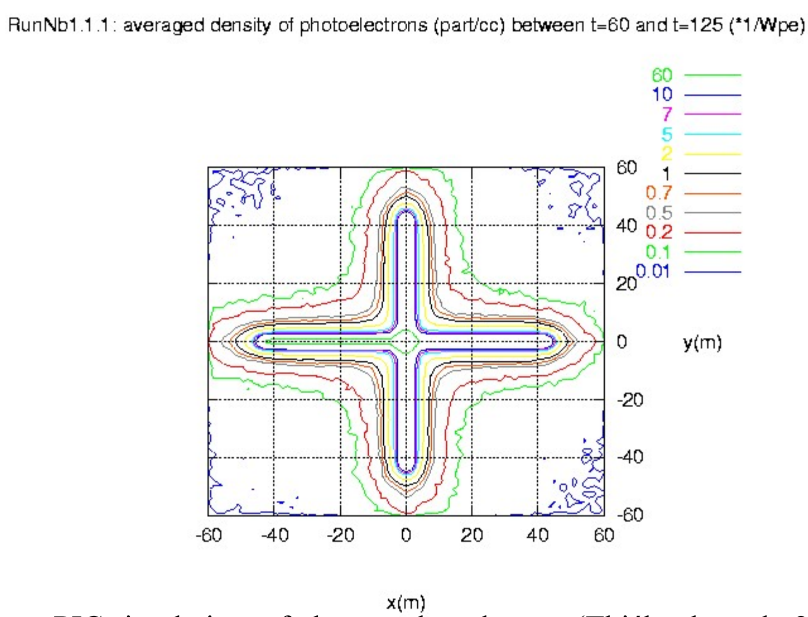

PIC simulation of photo-e along booms (Thiébault et al., 2003)

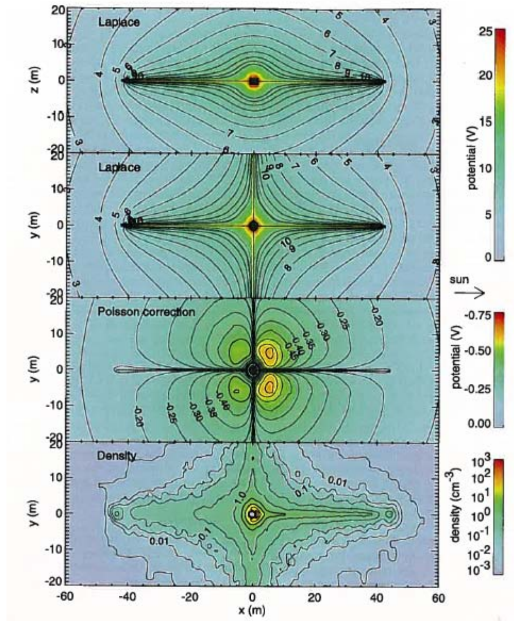

boom potential effect (Cully et al., 2007)

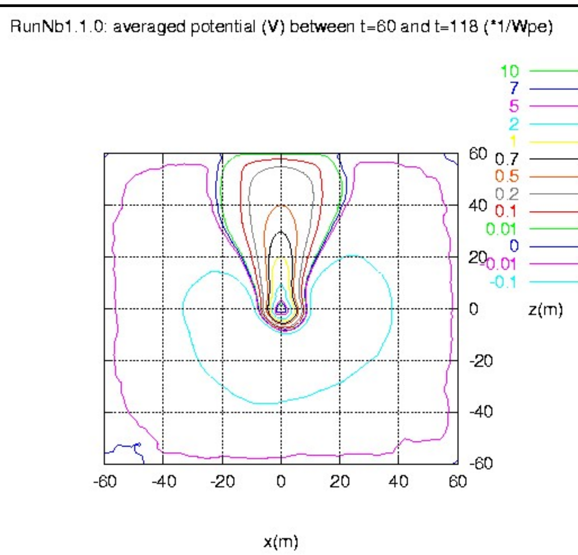

Preliminary results of potential distribution around an ASPOC like ion plume on a cylindrical spacecraft (Thiébault et al., 2003).

Conclusion

- The turning point formulation has been used for simulating photo-electron sheath in a large Debye length regime.
- Predictions of potential barrier is consistent with the observations made on Geotail spacecraft by Zhao et al. for what regards the magnitude of the barrier.
- There is a discrepancy, however, for what regards the barrier location.
- Examination of Zhao et al.'s hypotheses leads to conclude that our predictions are more realistic.

Simulation of the Cluster Spacecraft Floating Probe Potential

Benoit Thiébault and Alain Hilgers

Space Environments and Effects Section (ESA-ESTEC/TEC-EES),

Keplerlaan 1, 2200 AG Noordwijk, The Netherlands

Arnaud Masson, Philippe Escoubet and Harri Laakso

Space Science Department (ESA-ESTEC),

Keplerlaan 1, 2200 AG Noordwijk, The Netherlands

Spacecraft Potential in the magnetosphere

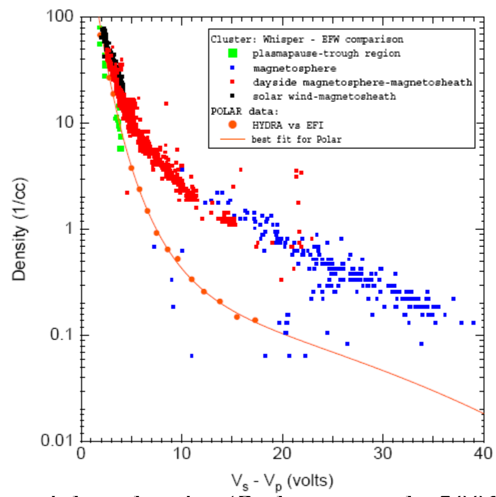

spacecraft potential vs density (Pedersen et al., 2001)

Ambient current

- In the two limiting cases expressed above, the current collected on a spherical conductor from ambient particles of charge q can be expressed as:
- $$\begin{cases} q\phi > 0 \Rightarrow I_q = n_q \times V_q \times q \times S \times \exp\left(-\dfrac{q\phi}{kT_q}\right) \\ q\phi < 0 \Rightarrow I_q = n_q \times V_q \times q \times S_{eff} \end{cases}$$
- OML regime Mott-Smith and Langmuir [1926]
- $$S_{eff} = S \times \left(1 - \frac{q\phi}{kT_q}\right)$$

Photo-electron current

$$\begin{cases} \phi \le 0 \Rightarrow I_{ph} = J^0_{ph} \times S_{ph} \\ \phi > 0 \Rightarrow \begin{cases} \chi = \dfrac{r_{SC}}{r_0 - r_{SC}} << 1 \Rightarrow I_{ph} = J^0_{ph} \times S_{ph} \times \left(1 + \dfrac{e\phi}{kT_{ph}}\right) \exp\left(-\dfrac{e\phi}{kT_{ph}}\right) \\ \chi = \dfrac{r_{SC}}{r_0 - r_{SC}} >> 1 \Rightarrow I_{ph} = J^0_{ph} \times S_{ph} \exp\left(-\dfrac{e\phi}{kT_{ph}}\right) \end{cases} \end{cases}$$

Table 1:

Cluster model parameters

Plasma temperature:	0.1 to 3 eV
Plasma density:	0.1 to 1000 part/cm^3
Cylindrical spacecraft radius	1.45 m
Cylindrical spacecraft height	1.3 m
Equivalent spherical spacecraft radius	1.41 m
Spherical probe radius	0.04 m
Probe bias current	140 nA
Photoelectron saturation current density	56 μA/m^2
Number of probes with bias current	4

Fit of data with Bi-Maxwellian

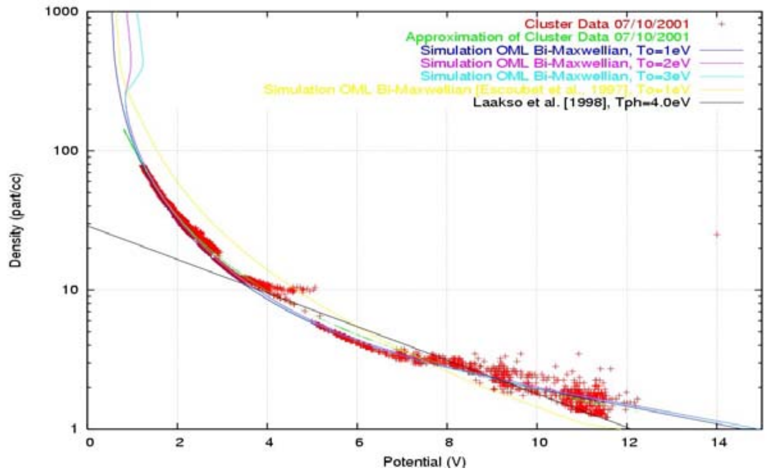

Fit of data with bi-Maxwellian

(Thiebault et al., IEEE TPS, 2006)

Ambient temperature (eV)	Toph (eV)	Joph (μA/m)	T1ph (eV)	J1ph(μ A/m^2)	Total saturation current (μA/m^2)
0.5	1.3	40.0	8.0	6.5	46.5
0.8	1.3	45.0	8.0	5.5	51.5
0.9	1.3	48.0	8.0	5.3	**53.3**
1.0	1.3	55.0	8.0	5.0	**60.0**
2.0	1.3	65.0	8.0	4.0	69.0
3.0	1.3	75.0	8.0	3.5	78.5

Effect of Ambient Electron Temperature

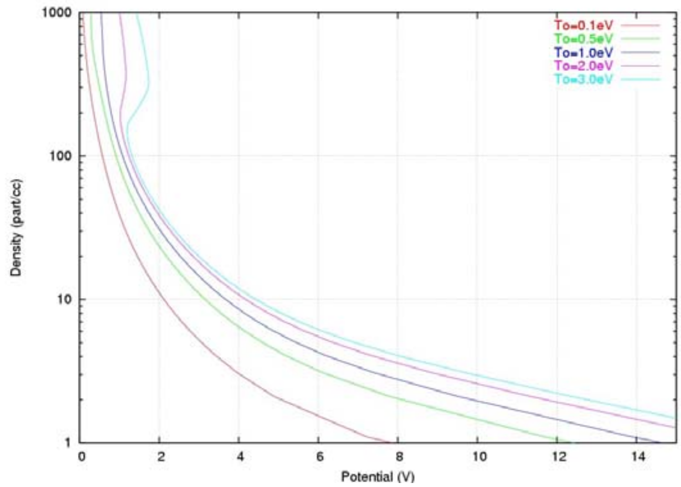

SPINE, 13-14 Nov. 2008, ESTEC

Evidence of photo-electron cross-over

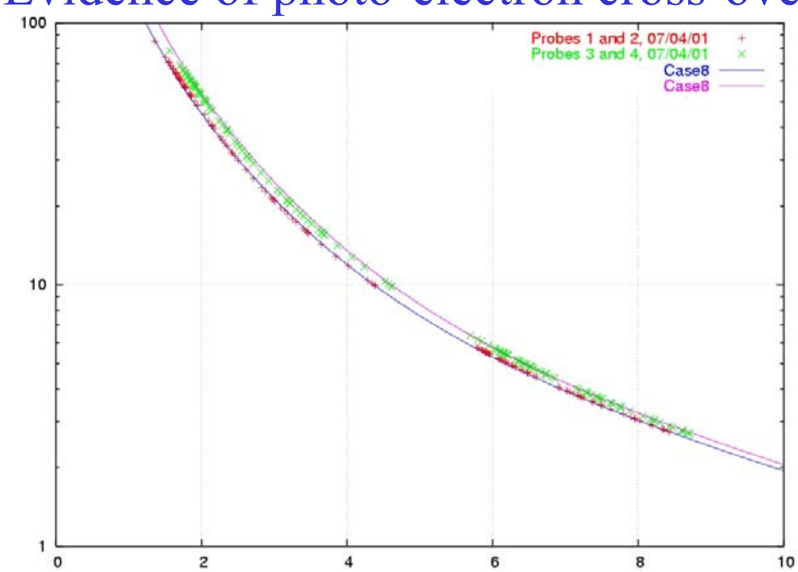

SPINE, 13-14 Nov. 2008, ESTEC

More detailed modelling required

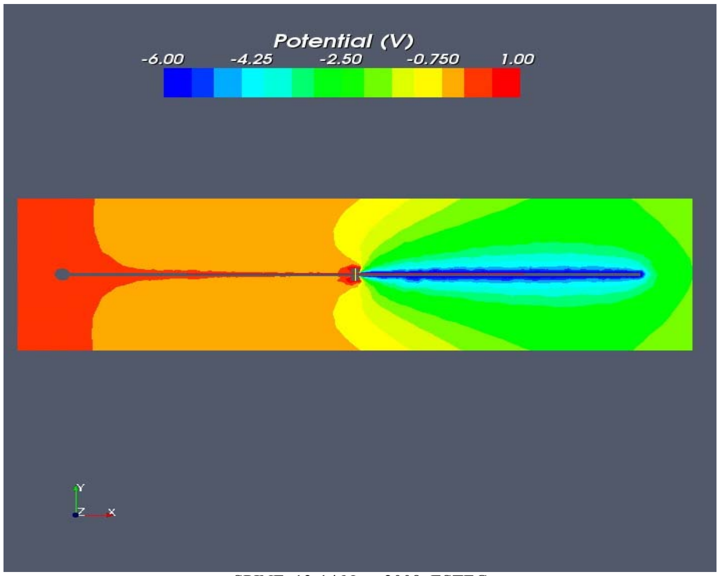

SPINE, 13-14 Nov. 2008, ESTEC

SPIS modelling

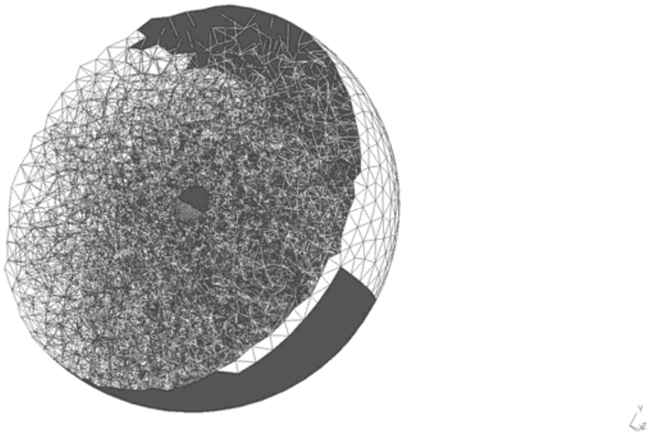

SPINE, 13-14 Nov. 2008, ESTEC

Current collected by Sphere

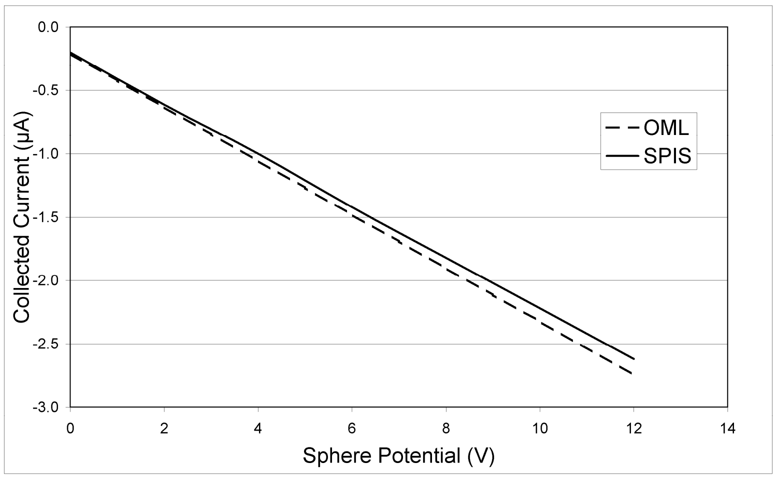

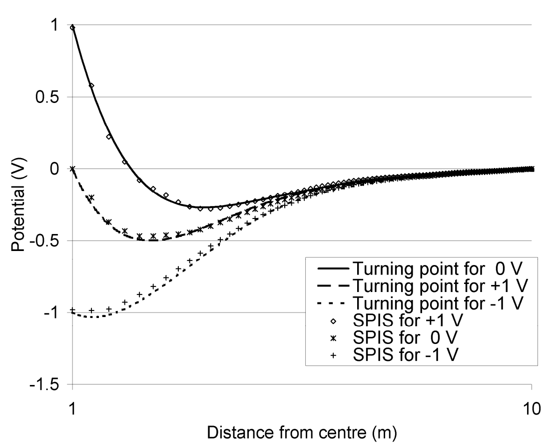

Conclusion

- Current limitations include:
- Models are validated in stationnary regime
- Uncertainty of the order of a few percents in current collected on a sphere.
- Certainly worse on a wire.
- Resolve both wire scale and spacecraft sheath scale.

References

- C. Cully, R. E. Ergun, and A. I. Eriksson. Electrostatic structure around spacecraft in tenuous plasmas. *J. Geophys. Res.*, accepted for publication, June 2007.
- Thiébault, B., A. Hilgers, E. Sasot, H. Laakso, P. Escoubet, V. Génot, and J. Forest, Potential barrier in the electrostatic sheath around a magnetospheric spacecraft, J. Geophys. Res., Vol. 109, No. A12, 2004.
- Thiébault, B., A. Hilgers, A. Masson, P. Escoubet and H. Laakso, Simulation of the Cluster Spacecraft Floating Probe Potential, IEEE Trans. Plasma Sci, Vol 34, No5, pp 2078- 2083, DOI 10.1109/TPS.2006.883407, Oct 2006.
- Thiébault, B. A. Hilgers, Forest, J., Escoubet, P., Fehringer, M. Laakso, H., Modelling of the photo-electron sheath around an active magnetospheric spacecraft, in Proceedings of the 8th Spacecraft Charging Technology Conference, Huntsville, AL, USA, October 20-24, 2003, NASA/CP-2004-213091.
- Zhao et al., 1996. H Zhao, R. Schmidt, C.P. Escoubet, K. Torkar and W. Riedler, Self-consistent Determination of the Electrostatic Potential Barrier due to the Photoelectron Sheath near a Spacecraft. *J. Geophys. Res.* 101 A7 (1996), pp. 15653–15659.